Nanoscale Mechanics: A Quantum-Continuum Approach

V.Venkatasubramanian[a] and S.Bharath[b]

[a] *Department of Mechanical Engineering, IIT Madras*
[b] *Department of Chemical Engineering, IIT Madras*

1. Introduction

With the confluence of interest in nanotechnology, the availability of experimental tools to synthesize and characterize systems in the nanometer scale, and computational tools widely accessible to model microscale systems by coupled continuum/molecular/quantum mechanics, we are poised to unravel the traditional gap between the atomic and the macroscopic world in mechanics and materials.

Nanoscale materials are used in conjunction with other larger components which have different response times. Hence, a treatment of such systems involves calculations with different time and length scales. Single scale methods such as "ab initio" quantum mechanical methods or molecular dynamics (MD) will have difficulty in analyzing such hybrid structures due to the limitations in terms of the time and length scales. Classical molecular dynamics simulations have become prominent as a tool for elucidating complex physical phenomena because of the availability of accurate interatomic potentials for a range of materials. However, the length and time scales that can be probed using molecular dynamics are still fairly limited.[1]

The study of nanoscale mechanics and materials requires a scaling up to the order of several microns, consisting of billions of atoms. Such large systems cannot be handled by molecular dynamics simulations to-date. Hence, there is a need for the development of multi-scale approaches. One possible approach that can be applied is to use molecular dynamics only in localized regions where the atomic-scale dynamics are important, and a continuum simulation method everywhere else. In particular, these methods do not satisfactorily address the issue of disparate time scales in the two regions, and provide a rather simplified treatment of the interface between the atomistic and continuum regimes.[1]

This treatment promises to enable the study of nanoscale systems such as nanocomposites, carbon nanotubes, nanoalloys, nanowires and nano-fluidic devices.

2. Molecular dynamics

Molecular dynamics simulation numerically solves Newton's equations of motion on an atomistic or similar model of a molecular system to obtain information about its time-dependent properties. It has been used to calculate the collective or average thermochemical properties of various physical systems.[1]

There are two basic assumptions made in standard molecular dynamics simulations:

- Molecules or atoms are described as a system of interacting material points, whose motion is described dynamically with a vector of instantaneous positions and velocities. The atomic interaction has a strong dependence on the spatial orientation and distances between separate atoms. This model is often referred to as the soft sphere model, where the softness is analogous to the electron clouds of atoms.

- No mass changes in the system. Equivalently, the number of atoms in the system remains the same.

The simulated system is usually treated as an isolated domain system with conserved energy. However, non-conservative techniques which model the dissipation of the kinetic energy into the surrounding media prove useful in the multiple-scale simulation methods.

The molecular dynamics simulation is most typically run with reference to a Cartesian coordinate system.
.
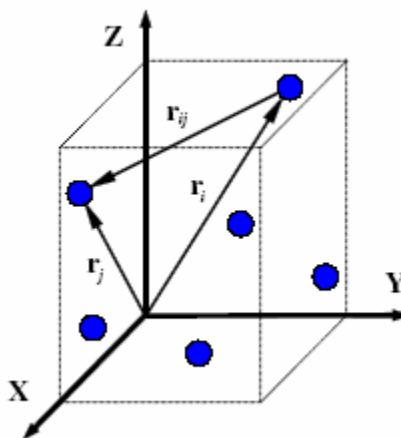
Fig. 1. Coordination in atomic systems[1]

The equation of motion of a system of interacting particles, can be written in terms of a Lagrangian function L as,

$$\frac{d}{dt}\frac{\partial L}{\partial \dot{r}_i} - \frac{\partial L}{\partial r_i} = 0, \quad i = 1, 2, \ldots, N.$$

Here, $r_i = (x_i, y_i, z_i)$ is the radius vector of atom i, Fig. 1, and N is the total number of simulated atoms. The spatial volume occupied by these N atoms is usually referred to as the molecular dynamics domain.

In order to provide identical equations of motions in all inertial coordinate systems, the Lagrangian function must also comply with the Galilean invariance principle. Due to the homogeneity of time and space, and also isotropy of space in inertial coordinate systems, the equations of motion must be independent of the choice of initial time of observation, the origin of the coordinate system, and directions of its axes. These basic principles are equivalent to the requirements that the Lagrangian function cannot explicitly depend on time, directions of the radius and velocity vectors, and it can only depend on the absolute value of the velocity vector.[1]

Interaction between the particles can be incorporated by adding a potential term to the Lagrangian function. This potential term can be quite complicated and may not represent the interactions accurately. The nature of this interaction is due to quantum effects which govern the valence, bond energy and the topology of the system.[1]

$$L = \sum_{i=1}^{N} \frac{m_i \dot{r}_i^2}{2} - U(\mathbf{r}_1, \mathbf{r}_1, \ldots, \mathbf{r}_N)$$

There are several forms of the potential term that can be employed for molecular dynamics simulations. The most commonly employed 12-6 potential is the Lennard-Jones Potential which has the form below.[1]

$$V(\mathbf{r}_i, \mathbf{r}_j) = V(r) = 4\varepsilon \left[\left(\frac{\sigma}{r}\right)^{12} + -\left(\frac{\sigma}{r}\right)^{6} \right], \quad r = |\mathbf{r}_{ij}| = |\mathbf{r}_i - \mathbf{r}_j|.$$

The first term represents the atomic repulsion dominating at small distances and the second term represents the attraction between the atomistic pair.

The three-body potentials fail to describe the energetics of all possible bonding geometries, while a general form for a four and five-body potential contains too many free parameters. As a result, a variety of advanced two-body potentials

have been proposed to efficiently account for the specifics of a local atomistic environment by incorporating some particular multi-body dependence.

Limitations

The major drawback of molecular dynamics is that the length and time scales that can be probed are still fairly limited. Efficiency and accuracy are the two most important criteria guiding the development of simulation methods. Both depend on the complexity of the interatomic potentials, the degrees of freedom of the system and the time-integration algorithms used in the simulation. With the computational power available today, a typical molecular dynamics simulation domain contains several millions of atoms. Consequently, molecular dynamics simulations have their own limitations with respect to boundary conditions, time steps and incorporation of temperature effects.[1]

3. Modeling of nano-indentation:

The workpiece and a tool are assumed to consist of Copper and Diamond respectively. The periodic boundary conditions are used in the transverse direction (x direction).
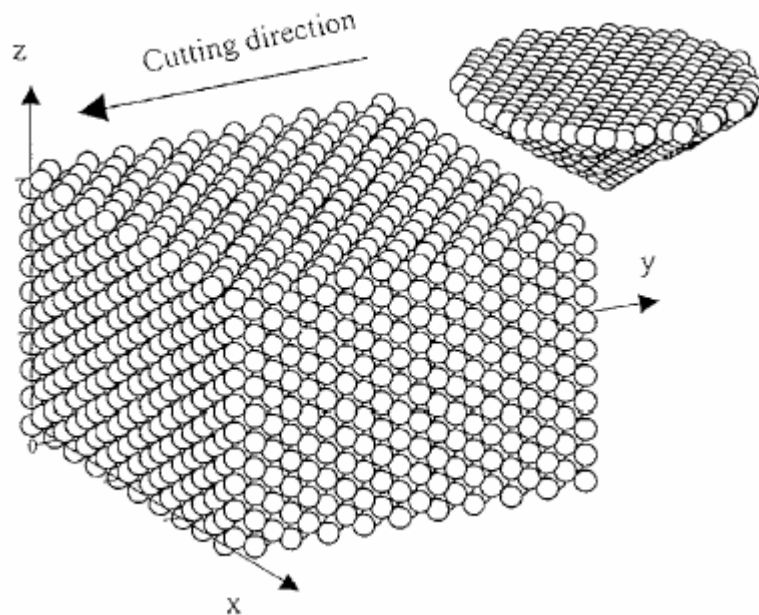
Figure 2. Molecular dynamics simulation model[2]

The force acting on an individual atom is modeled using a Morse potential. The form of the Morse potential is

$$\phi(r_{ij}) = D\{\exp[-2\alpha(r_{ij} - r_0)] - 2\exp[-\alpha(r_{ij} - r_0)]\}$$

where $\phi(r_{ij})$ is a pair potential energy function, D, α, and r_0 correspond to the cohesion energy, the elastic modulus and the atomic distance at equilibrium, respectively.[2]

The shape of the Morse potential is shown in Fig. 3. The force acting on the ith particle is calculated as the gradient of the Morse potential.

$$F_i = -\sum_{\substack{j-1 \\ (j \neq i)}}^{N} \nabla_i \phi(r_{ij}) = m_i \frac{d^2 r_i(t)}{dt^2}$$

where F_i is the resultant force on atom i, m_i is the mass of atom i, r_i is the position of atom i, and N is the total number of atoms.
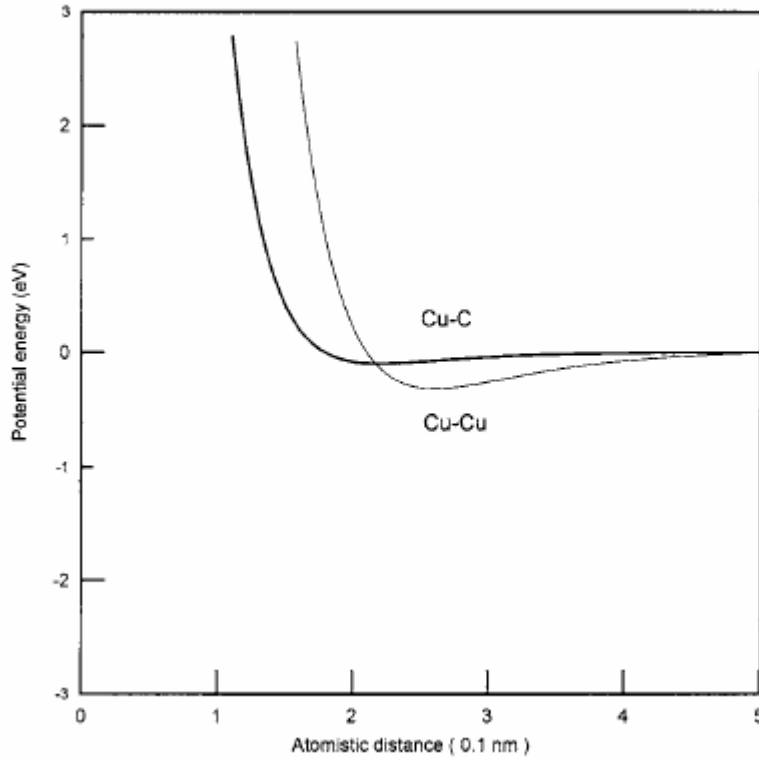
Figure 3. Shape of various Morse-type potentials

The initial displacements of the copper atoms in the workpiece material are obtained from its lattice structure. Initial velocities are assigned from the Maxwell distribution, and the magnitudes are adjusted so as to keep the temperature in the system constant according to

$$v_i^{new} = \left\{ \frac{N_f N k_B T_0}{2} \left[\sum_{i=1}^{N} \frac{m_i(v_i^{old})^2}{2} \right]^{-1} \right\}^{\frac{1}{2}} v_i^{old}$$

where v_i is the velocity of atom i, T_0 is a specified temperature, k_B is Boltzmann's constant, and N_f is the number of degrees of freedom of the system.

The ratio of the cutting force to the thrust force is defined as coefficient of resistance f, i.e. $f' = F_y/F_z$. Here, F_y and F_z are the cutting force in the y-direction and the thrust force in the z-direction on the tool respectively. This coefficient can be used to measure the machinability and resistance of cutting on the atomic scale.[2]
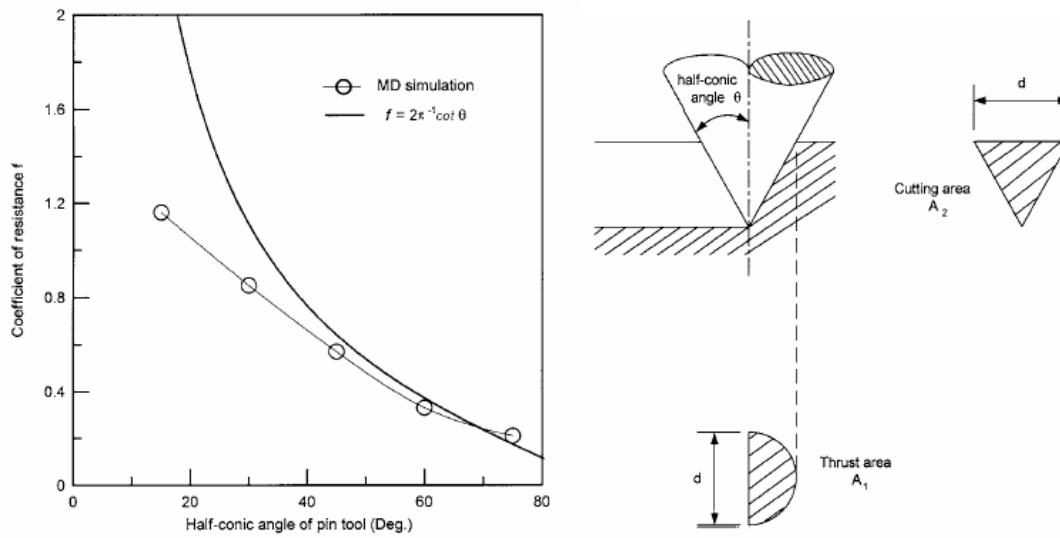
Figure 4.
(a) The relationship between the coefficient of resistance and the angle of the pin tool.
(b) The map in the grooving produced by a pin tool which cut on a softer metal.[2]

The cutting area A_2 and thrust area A_1 are worked out using elementary geometry principles.

$$A_1 = \frac{\pi d^2}{8}$$

$$A_2 = \frac{d^2}{4} \cot \theta$$

$$f' = \frac{F_y'}{F_z'} = \frac{A_2}{A_1} = \frac{2}{\pi} \cot \theta$$

Molecular dynamics results deviate from f′ when θ is below 45° as a result of the accumulation of atoms in front of the pin. This increases the density, with corresponding increase in resistance and thus increasing the cutting force required to maintain a constant cutting velocity. It is noted particularly that the coefficient of resistance on the micro-scale is the result of average forces, and it neglects the pile-up of material ahead of the pin tool and the crumpling and accumulation of material around the grooving path. The cutting mechanism is thus revealed on the atomic scale. Under 90°, molecular dynamics simulation should be used.[2]

(a) 10ps   (b) 20ps

(c) 35ps   (a) 50ps
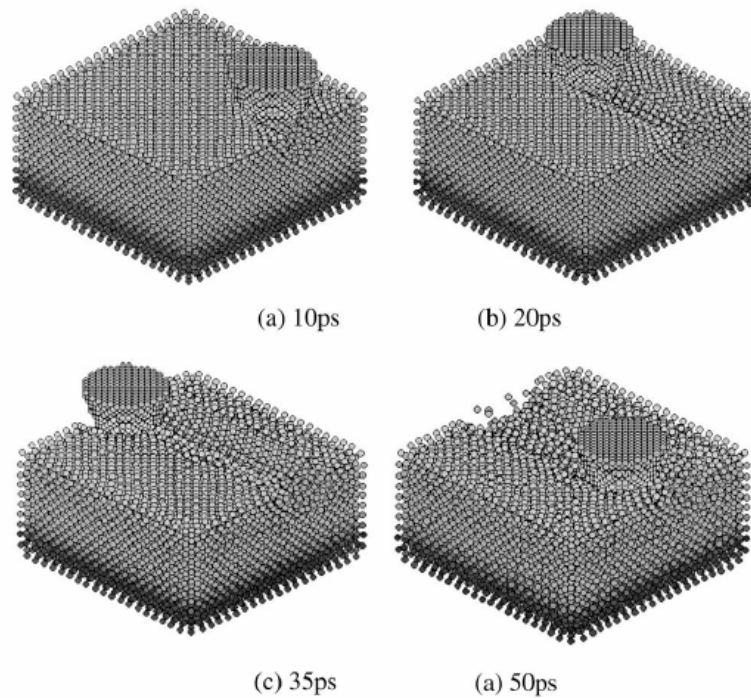
Figure 5. Behavior of nano-lithography process at different time steps: (a) 10 ps; (b) 20 ps; (c) 35 ps; (d) 50 ps.[3]

The stick phenomenon results from an increasing accumulation of material ahead of the pin tool, and an increasing adhesive effect between pin and workpiece material as the area of contact increases. The slip phenomenon occurs when the debris crumples. Figure 6 shows the variation of the cutting forces with the time step. The simulated model is seen in Figure 5 for various time steps.
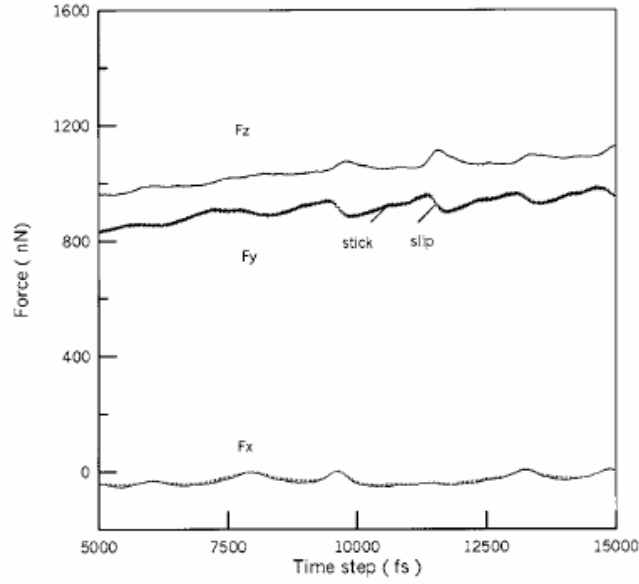
Figure 6. Variation of cutting forces and stick–slip phenomenon.[2]

This simulation evaluates the effect of the geometry of the pin tool on the cutting mechanism and shows that this effect has a significant influence on the degree of the machinability.

4. Molecular mechanics approach for modeling properties of carbon nanotube

Atomic interactions become crucial during the investigation of mechanical properties at near molecular scales. Quantum and molecular mechanics aim to correlate the atomic positions to the system energy. The quantum mechanics approach predicts the energy of the system based on the calculations of the electronic structure of molecules. Due to cumbersome calculations, it is preferred to neglect the electronic structure by applying the Born-Oppenheimer approximation. This is the basis for the molecular mechanics approach where the energy is defined only as a function of the nuclear positions irrespective of the electronic structure. [4]

Here a molecular mechanics approach is used to analytically predict the size dependant properties of a carbon nanotube. The total system potential energy can be expressed as sum of individual energy terms as,

$$E_t = U_\rho + U_\theta + U_\omega + U_\tau + U_{vdW} + U_{es}$$

where U_ρ, U_θ, U_τ, and U_ω are energies associated with bond stretching, angle variation, inversion and torsion, respectively; U_{vdW} and U_{es} are associated with

van der Waals and electrostatic interactions. A schematic representation of the electronic structure of a graphene sheet illustrating source of each energy term is shown in the Figure 7.
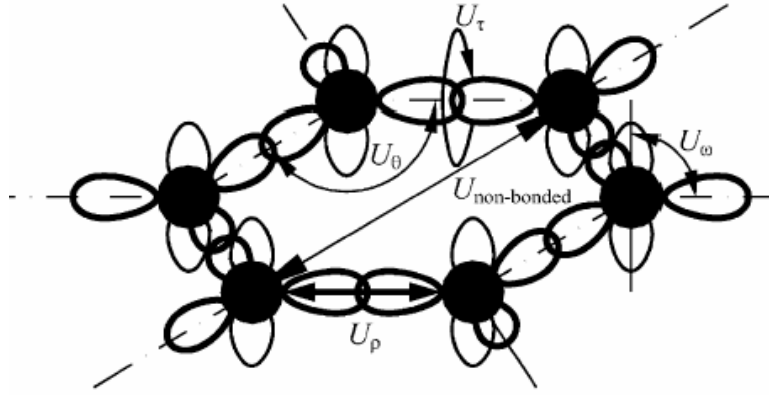
Figure 7. Bond structures and corresponding energy terms in a graphene cell.[4]

The bond stretching energy U_ρ, can be described using many models. Very accurate models like the three parameter morse potential model can be used. But in most cases, harmonic energy functions suffice. The angle variation U_θ and the inversion energy U_ω are also described by harmonic functions as,

$$U_\rho = \frac{1}{2} \sum_i K_i (dR_i)^2$$

$$U_\theta = \frac{1}{2} \sum_j C_j (d\theta_j)^2$$

$$U_\omega = \frac{1}{2} \sum_k B_k (d\omega_k)^2$$

where, K_i, C_j, B_k are the force constants for bond stretching, angle varience and angle inversion. dR_i, $d\theta_j$ and $d\omega_k$ are the variance in the bond i, bond angle j and the inversion angle k.

The torsional energy in molecular mechanics is primarily used to correct the remaining energy terms rather than to represent a physical process. The torsional energy is modeled by a cosine series.

$$U_\tau = \frac{1}{2} \sum_i A_i [1 + \cos(n_i \tau_i - \phi_i)]$$

where A_i is the "barrier" height to rotation of bond i; n_i is the multiplicity which gives the number of minima in the function as the bond is rotated through 2π. Non-bonding energies such as the electrostatic force and van der Waals force are modeled using Coulomb's law and 12-6 Lennard-Jones potential respectively.[4]

4.1. Analytic approach for modeling single walled carbon nanotubes

For a single-walled carbon nanotube subjected to axial loadings at small strains, torsion, inversion, van der Waals and electrostatic interactions are negligible. Thus in such cases, the bond stretching and the angle variation terms are the most significant in the potential energy of the system, i.e.

$$E_t = \frac{1}{2}\sum_i K_i(\mathrm{d}R_i)^2 + \frac{1}{2}\sum_j C_j(\mathrm{d}\theta_j)^2$$

A armchair carbon nanotube subjected to a longitudinal tensile stress as shown is considered. In this configuration, there are three chemical bonds a, b, b and three bond angles α, β, β associated with each atom.(Figure 8) The longitudinal external tension stress will result in a bond elongation db and two bond angle variances dα and dβ.
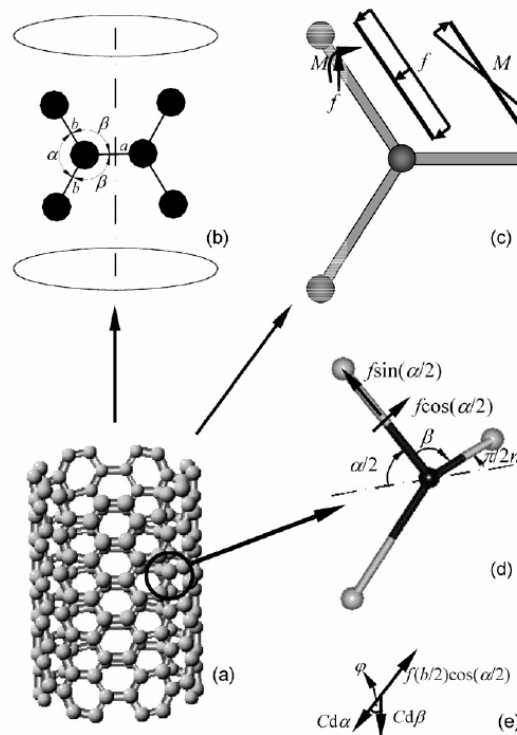
Figure 8. (a) Schematic illustration of a (n, n) carbon nanotube, (b) nomenclature, (c) force and moment distributions in stick b when the tube subjected to an axial tensile stress, (d) equivalent forces exerted on the right half of stick b by the left half, (e) moment equilibrium.[4]

Consider the force and moment in stick b as shown. We denote the force contributed by bond b along the external tension direction as f so that the total axial force on the nanotube is 2nf. Force equilibrium of bond extension leads to

$$f \sin(\alpha/2) = K \, db.$$

The total moment resulting from bond angle distortion in plane b–b can be expressed by $(C \, d\alpha + C \, d\beta \cos\varphi)$, where C is the couple per unit twist and φ, the torsion angle between planes b–b and a–b, can be calculated by

$$\cos \varphi = \frac{\tan(\alpha/2)}{\tan \beta}$$

Hence, the moment balance equation is,

$$f(b/2)\cos(\alpha/2) = C \, d\alpha + C \, d\beta \cos \varphi.$$

Using geometric relations, these expressions can be simplified to develop an analytic expression for Young's modulus and Poisson's ratio.[4]

$$Y = \frac{K}{t \sin(\alpha/2)[1 + \cos(\alpha/2)][\lambda(Ka^2/C)\cot^2(\alpha/2) + 1]},$$

$$v = \frac{\cos(\alpha/2)(\lambda Ka^2/C - 1)}{[1 + \cos(\alpha/2)][\lambda(Ka^2/C)\cot^2(\alpha/2) + 1]},$$

where

$$\lambda = \frac{\cot(\alpha/2)\sin \beta}{4 \cot(\alpha/2)\sin \beta - 2 \cos(\pi/2n) \cot \beta \sin (\alpha/2)}$$

The comparison of the analytic expressions developed with previous experimental results show good correlation as seen in Fig. 9.

(a)
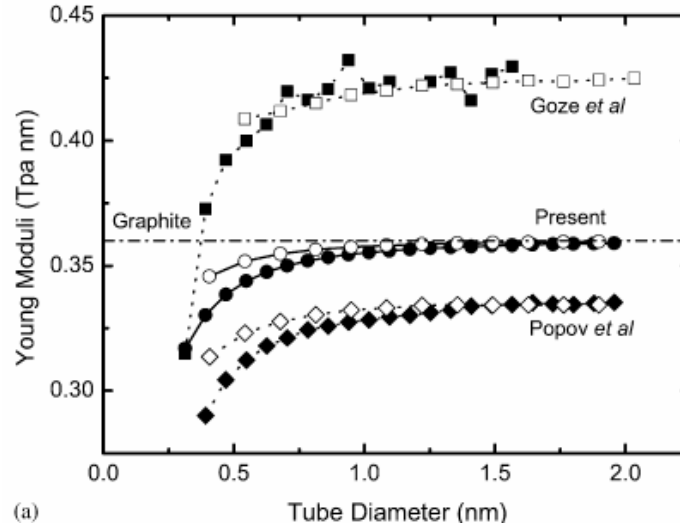
Figure 9. .Comparison between the predictions from the present model with existing results (Popov et al[6]) on the size-dependence of Young's modulus[4]

5. Continuum Mechanics approach

A nanoscale continuum theory is established based on the higher order Cauchy–Born rule to study the mechanical properties of carbon nanotubes. The theory bridges the microscopic and macroscopic length scale by incorporating the second-order deformation gradient into the kinematic description. The interatomic potential and the atomic structure of carbon nanotube are incorporated into the constitutive model. Therefore carbon nanotube can be viewed as a macroscopic generalized continuum with microstructure.[5]

5.1 Cauchy–Born rule for crystal films

Cauchy–Born rule is a fundamental kinematic assumption for linking the deformation of the lattice vectors of crystal to that of a continuum deformation field. This rule can be applied to systems without diffusion, phase transitions, lattice defect, slips or other non-homogeneities. Figures 10 and 11 represent the Cauchy born principle and its application to curved surfaces respectively.
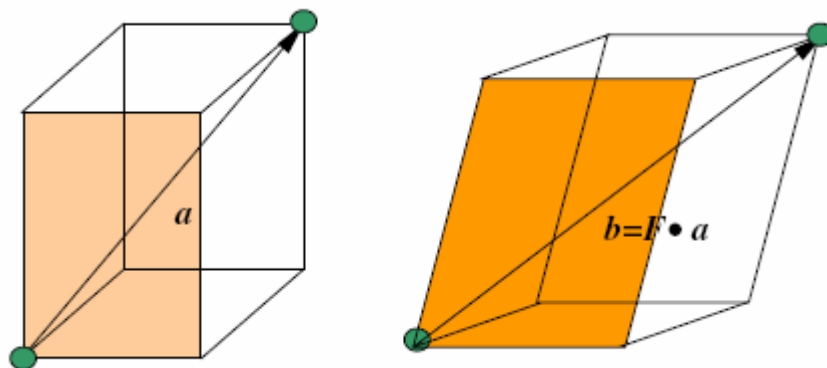
Figure 10. Illustration of Cauchy-Born principle[5]
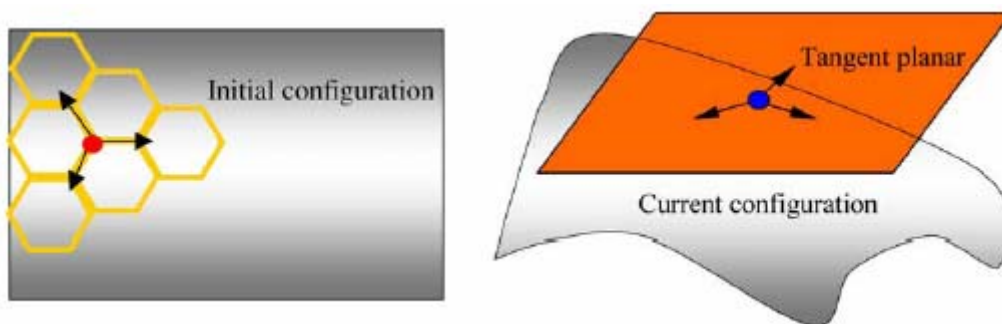
Figure 11. Cauchy-Born rule applied directly to curved films[5]

From the classical nonlinear continuum mechanics point of view, the deformation gradient tensor F is a linear transformation, which only describes the deformation of an infinitesimal material line element dX in the undeformed configuration to an infinitesimal material line element dx in deformed configuration. By taking the finite length of the initial lattice vector into consideration, the corresponding deformed lattice vector should be expressed as

$$b = \int_0^a F(s) \, ds$$

Assuming that the deformation gradient tensor is smooth enough, a second order Taylor expansion is used.

$$F(s) = F(0) + \nabla F(0) \bullet s + \nabla\nabla F(0) : (s \otimes s)/2 + O(\|s\|^3)$$

Using the deformation gradient, we get the deformed lattice vector as

$$b \approx F(0) \bullet a + \tfrac{1}{2}\nabla F(0) : (a \otimes a)$$

This gives better accuracy as compared to the standard Cauchy-Born rule. The accuracy can be enhanced by using more higher order terms.[5]
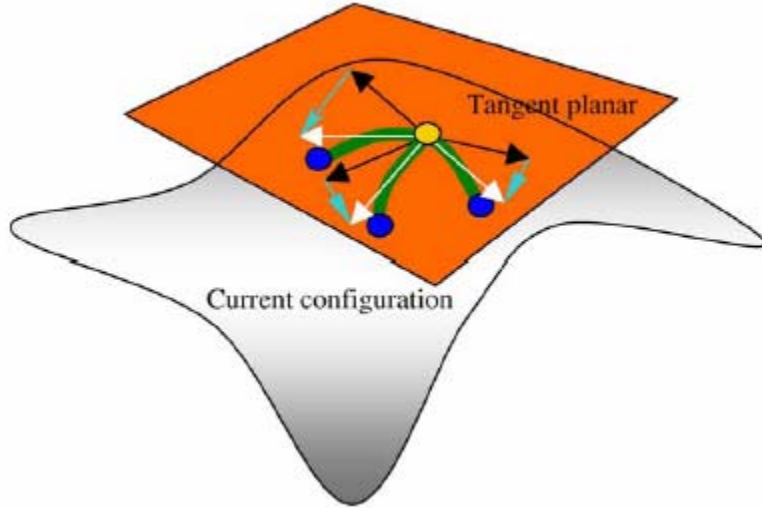
Figure 12. Higher order Cauchy-Born rule applied directly to curved films[5]

A hyper-elastic constitutive model is developed based on the higher-order Cauchy-Born rule. Assuming that the energy can be homogenized over a representative volume in the undeformed configuration, the strain energy can be expressed as

$$W_0 = W_0(|r_{I1}|, |r_{I2}|, |r_{I3}|) = \sum_{J=1}^{3} V_{IJ}(r_{I1}, r_{I2}, r_{I3})/2V_I = W_0(F, G)$$

$$r_{IJ} = F \bullet R_{IJ} + G : (R_{IJ} \otimes R_{IJ})/2$$
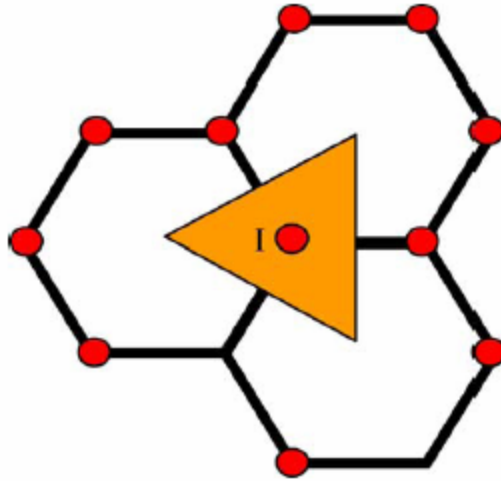
Figure 13. Representative cell corresponding to an atom I.[6]

A planar graphite sheet in equilibrium energy state is defined as the undeformed configuration. The current configuration of the nanotube can be seen as a deformed state from the initial configuration by the following mapping:

$$x_1 = X_1, \quad x_2 = R \sin\frac{X_2}{R}, \quad x_3 = R \cos\frac{X_2}{R} - R$$

where (X_1, X_2) are the material coordinates of a point in the undeformed configuration and (x_1, x_2, x_3) are its images in the current configuration. R is the radius of the modeled single walled carbon nanotube, which is described by a pair of parameters (n,m). The radius R can be evaluated by

$$R = a\sqrt{m^2 + mn + n^2}/2\pi \text{ with } a = a_0\sqrt{3},$$

where, a_0 is the equilibrium bond length distance in the graphene sheet.[5]

The energy per atom as the function of diameters for armchair and zigzag single walled carbon nanotubes relative to that of the graphite sheet is calculated. It is shown that the trend is almost the same for both armchair and zigzag configurations. The energy per atom decreases with increase of the tube diameter with $E(D)-E(\infty) = O(1/D^2)$, where $E(\infty)$ represents the energy per atom for graphite sheet.[5]

Figure 13 compares the energies of the armchair and zigzag configurations relative to predicted from the current model with other models.
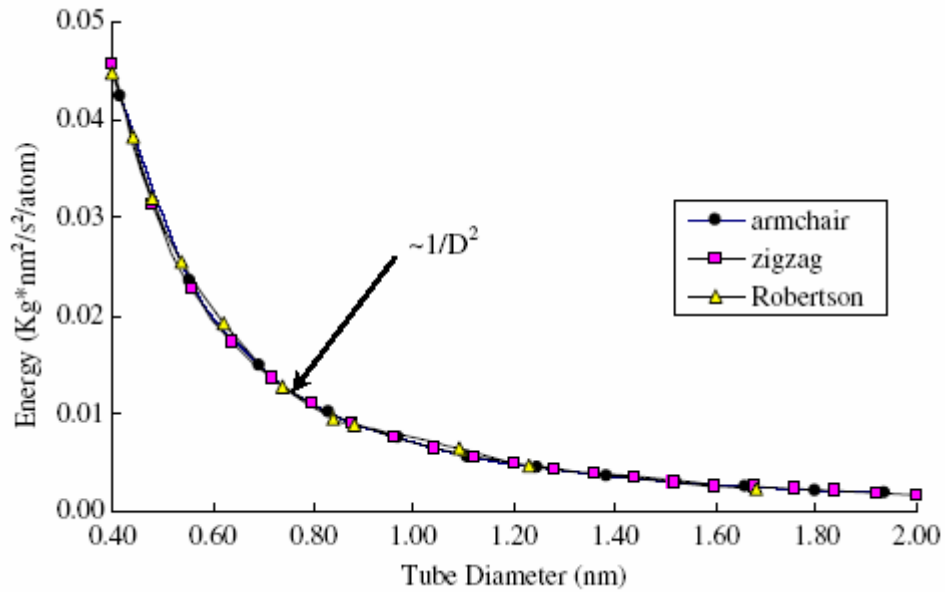
Figure 13. The energy (relative to graphite) per atom versus tube diameter.[5]

(a)
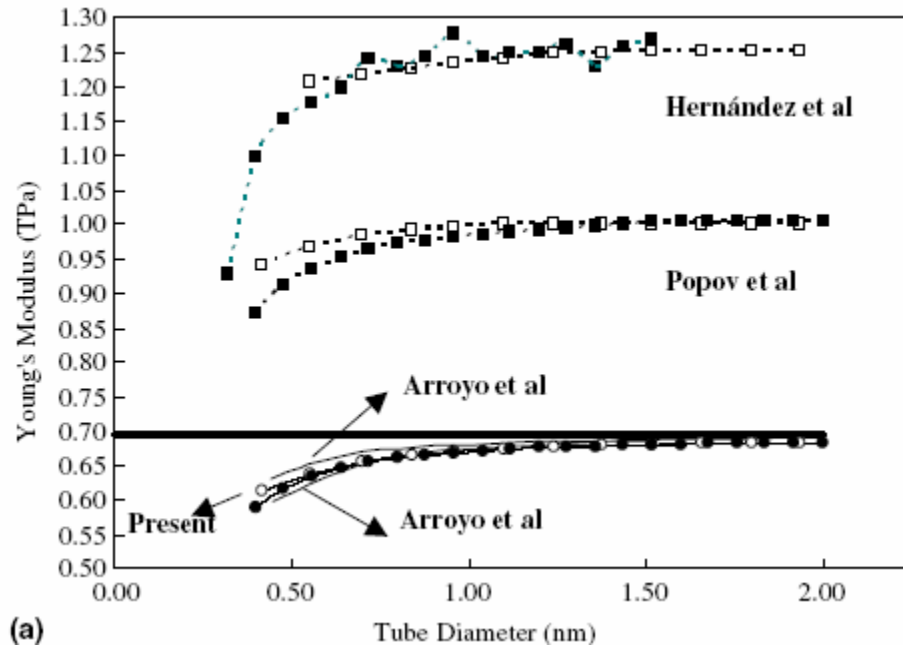
Figure. 14. Comparison between the results obtained with different methods Young's modulus Open symbols denote armchair, solid symbols denote zigzag. Dashed horizontal line denotes the results of graphite obtained with the present approach.[5]

As seen, the results agree well with those obtained by other experimental, atomic modeling and continuum concept based studies.

6. Bridging scale methods

The bridging scale consists of a two-scale decomposition in which the coarse scale is simulated using continuum methods, while the fine scale is simulated using atomistic approaches. The bridging scale offers unique advantages in that the coarse and fine scales evolve on separate time scales, while the high frequency waves emitted from the fine scale are eliminated using lattice impedance techniques. Fig. illustrates one such bridging scale technique involving molecular dynamics and finite element method.[8]
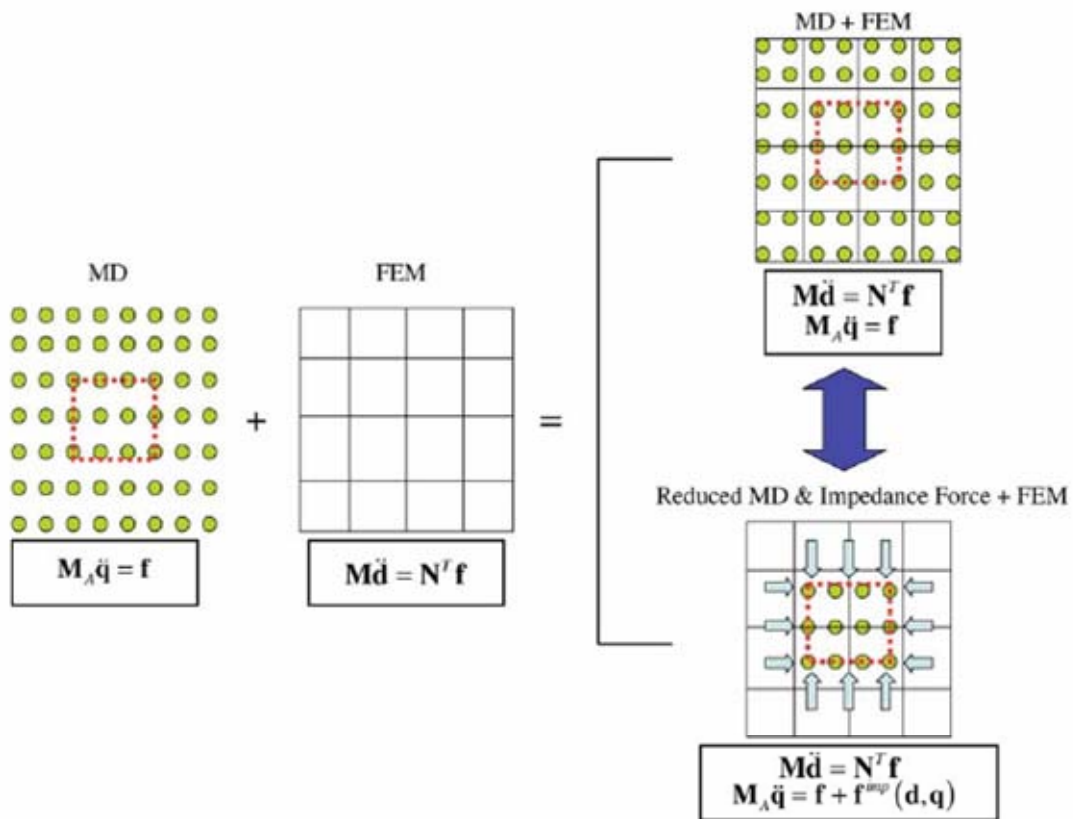
Figure 15. Schematic illustration of bridging scale.[8]

7. Conclusions

A molecular mechanics approach to nanoscale systems was studied and it was compared with continuum mechanics approach. It is observed that molecular mechanics approach underestimates the modulus of elasticity and continuum methods based on Cauchy-Born rule overestimate the modulus of elasticity. Further, the requirement of handling multiple time scales and length scales forces the usage of bridging methods to study nanoscale systems.

8. References

[1] W.K. Liu, E.G. Karpov, S. Zhang, H.S. Park, (2004), An introduction to computational nanomechanics and materials; Comput. Methods Appl. Mech. Engg **193**, 1529–1578.

[2] Te-Hua Fang and Cheng Weng; (2000) Three-dimensional molecular dynamics analysis of processing using a pin tool on the atomic scale; Nanotechnology, **11**, 148–153.

[3] Te-Hua Fang, Cheng Weng, Jee-Gong Chang; (2002); Molecular dynamics simulation of nano-lithography process using atomic force microscopy; Surface Science, **501**, 138–147.

[4] Tienchong Changa, Huajian Gaob, (2003) ; Size-dependent elastic properties of a single-walled carbon nanotube via a molecular mechanics model; Journal of the Mechanics and Physics of Solids, **51** , 1059 – 1074.

[5] X. Guo, J.B. Wang, H.W. Zhang; (2005), Mechanical properties of single-walled carbon nanotubes based on higher order Cauchy–Born rule; International Journal of Solids and Structures.

[6] Popov V.N., Van Doren V.E., Balkanski. M, (2000), Elastic properties of single-walled carbon nanotubes, Physical Review B **61**, 3078–3084.

[7] H.W. Zhang, J.B. Wang, X. Guo, (2005) , Predicting the elastic properties of single-walled carbon nanotubes, Journal of the Mechanics and Physics of Solids, **53**, 1929–1950.

[8] Wing Kam Liu, Harold S. Park, Dong Qian, Eduard G. Karpov, Hiroshi Kadowaki, Gregory J. Wagner; (2005), Bridging scale methods for nanomechanics and materials, Comput. Methods Appl. Mech. Engrg.

[9] G.J. Wagner, W.K. Liu, (2003), Coupling of atomistic and continuum simulations using a bridging scale decomposition, J. Comput. Phys. **190** ,249–274.